HHS Public Access

Author manuscript

Cell Host Microbe. Author manuscript; available in PMC 2016 April 08.

Published in final edited form as:

Cell Host Microbe. 2015 April 8; 17(4): 429–440. doi:10.1016/j.chom.2015.03.001.

Autophagy Mediates Tolerance to *Staphylococcus aureus* Alpha-Toxin

Katie Maurer[1,3], **Tamara Reyes-Robles**[2,3], **Francis Alonzo III**[4], **Joan Durbin**[5], **Victor J. Torres**[2,*], and **Ken Cadwell**[1,2,*]

[1]Kimmel Center for Biology and Medicine at the Skirball Institute, New York University School of Medicine, New York, NY 10016, USA

[2]Department of Microbiology, New York University School of Medicine, New York, NY 10016, USA

[3]Sackler Institute of Graduate Biomedical Sciences, New York University School of Medicine, New York, NY 10016, USA

[4]Department of Microbiology and Immunology, Loyola University Chicago Stritch School of Medicine, Maywood, IL 60153, USA

[5]Department of Pathology, Rutgers-New Jersey Medical School, Newark, NJ 07103, USA

SUMMARY

Resistance and tolerance are two defense strategies employed by the host against microbial threats. Autophagy-mediated degradation of bacteria has been extensively described as a major resistance mechanism. Here we find that the dominant function of autophagy proteins during infections with the epidemic community-associated methicillin-resistant *Staphylococcus aureus* USA 300 is to mediate tolerance rather than resistance. Atg16L1 hypomorphic mice (Atg16L1^{HM}), which have reduced autophagy, were highly susceptible to lethality in both sepsis and pneumonia models of USA300 infection. Autophagy confers protection by limiting the damage caused by α-toxin, particularly to endothelial cells. Remarkably, Atg16L1^{HM} mice display enhanced survival rather than susceptibility upon infection with α-toxin deficient *S. aureus*. These results identify an essential role for autophagy in tolerance to Staphylococcal

*Correspondence should be addressed to: Ken Cadwell, Ph.D., New York University School of Medicine, 540 First Avenue, Skirball Institute, Lab 210, New York, NY 10016, Phone: 212-263-8891, Fax: 212-263-7491, Ken.Cadwell@med.nyu.edu. Victor J. Torres, Ph.D., New York University School of Medicine, 522 First Avenue, Smilow Research Building, 1010, New York, NY 10016, Phone: 212-263-9232, Fax: 212-263-9180, Victor.Torres@nyumc.org.

AUTHOR CONTRIBUTIONS

K.M., V.J.T., and K.C. formulated the original hypothesis, designed the study, and analyzed results. K.M. performed the experiments. T.R. and F.A. III provided technical assistance and advice. J.D. analyzed histology. K.M. and K.C. wrote the manuscript, and all authors commented on the manuscript, data, and conclusions before submission.

COMPETEING FINANTIAL INTERESTS

The authors declare no competing financial interests.

disease and highlight how a single virulence factor encoded by a pathogen can determine whether a given host factor promotes tolerance or resistance.

INTRODUCTION

Host organisms can employ mechanisms of resistance or tolerance to defend against microbial threats (Medzhitov et al., 2012; Raberg et al., 2009; Schneider and Ayres, 2008). Resistance mechanisms lead to destruction of the microbial agent or reduction of its replicative capacity, and include numerous well-described cell autonomous and multicellular immune processes. In contrast, tolerance confers protection to the host by minimizing damage caused by the infection without affecting pathogen burden. Therapeutic strategies that enhance tolerance could replace or complement traditional means of prophylaxis such as antibiotics that inevitably select for resistant microorganisms (Raberg et al., 2009; Schneider and Ayres, 2008). Mouse models of cerebral malaria and sepsis following intestinal damage have demonstrated that tolerance can be improved independently of pathogen burden by directly or indirectly blocking $CD8^+$ T cell migration and cytokine production through the inflammasome, respectively (Ayres et al., 2012; Pamplona et al., 2007). However, these examples illustrate how tolerance mechanisms are context-specific because these immune effectors mediate resistance in other situations. Therefore, pathways that were previously considered to function primarily through resistance should be revisited and examined for their potential role in tolerance to clinically relevant pathogens.

Staphylococcus aureus infection is associated with a variety of diseases ranging from skin and soft tissue infection to lethal sepsis and nosocomial pneumonia. The spread of highly virulent and antibiotic-resistant strains such as methicillin-resistant *S. aureus* (MRSA) threatens to overwhelm the healthcare infrastructure, and as such, this bacterium has become one of the most important pathogens worldwide (Klevens et al., 2007). Many strains are also resistant to other therapeutic options currently available for patients, and newer treatments are often associated with adverse effects (Rodvold and McConeghy, 2014; Stryjewski and Corey, 2014). Understanding the relative contribution of tolerance versus resistance mechanisms during Staphylococcal disease could facilitate the development of novel therapeutic strategies and predict whether resistant bacteria will emerge in response to the treatment. Animal models have demonstrated that the battery of toxins produced by *S. aureus*, which can vary among different strains, accounts for much of the morbidity and mortality associated with infection (Alonzo and Torres, 2014; Berube and Bubeck Wardenburg, 2013; Bubeck Wardenburg et al., 2007a). Preventing tissue damage by neutralizing these toxins is a promising approach to ameliorate the impact of *S. aureus* infection (Alonzo and Torres, 2014; Berube and Bubeck Wardenburg, 2013; Bubeck Wardenburg et al., 2007a; Kennedy et al., 2010; Sampedro et al., 2014; Vandenesch et al., 2012).

Autophagy is a conserved cellular pathway by which cytosolic material is engulfed in a double-membrane vesicle, termed the autophagosome, and targeted to the lysosome for degradation and recycling (Levine and Kroemer, 2008). Autophagy has been extensively demonstrated to confer resistance to numerous bacterial pathogens through a variety of

innate and adaptive immune mechanisms, most notably the direct destruction of internalized bacteria residing in the cytosol or damaged vesicles (Gomes and Dikic, 2014). However, we previously demonstrated that autophagy-deficient mice display an unexpected enhanced innate immune response that increases resistance to the intestinal pathogen *Citrobacter rodentium* (Marchiando et al., 2013), suggesting that the role of autophagy during bacterial infections is more complex *in vivo* where multiple cell types and bacterial extracellular life cycles are involved. Additionally, autophagy could be contributing to tolerance mechanisms. Induction of autophagy has been shown to reduce lethality primarily through limiting damage following neuronal Sindbis virus infection and polymicrobial sepsis (Figueiredo et al., 2013; Orvedahl et al., 2010). These findings are consistent with the evolutionarily conserved cytoprotective function of autophagy and necessitate careful examination of this pathway in models of bacterial infection.

To investigate the role of autophagy at the whole organism level, we previously generated mice in which Atg16L1 expression is disrupted by the insertion of a gene-trap mutagenesis cassette (Cadwell et al., 2008). Atg16L1 is part of a protein complex that catalyzes the conjugation of phosphatidyl-ethanolamine to LC3, a necessary step in autophagosome formation; consequently, these Atg16L1 hypomorph ($Atg16L1^{HM}$) mice display reduced autophagy in all tissues examined (Cadwell et al., 2008; He et al., 2013; Hubbard-Lucey et al., 2014; Ju et al., 2009; Wang et al., 2012). Because these mice do not display obvious developmental abnormalities, they provide an opportunity to examine the function of autophagy during infectious disease without prior knowledge of the cell types involved. Here, we demonstrate that $Atg16L1^{HM}$ mice display increased lethality during epidemic community-associated methicillin-resistant *Staphylococcus aureus* USA300 blood and lung infection. Rather than reducing bacterial burden, we find that autophagy confers protection from α-toxin by limiting damage to endothelial cells. Remarkably, $Atg16L1^{HM}$ mice display enhanced survival rather than susceptibility upon infection with α-toxin deficient USA300, demonstrating that the role of autophagy is dependent on the expression of a single virulence factor. When taken together, these results identify autophagy-mediated protection from toxinosis as a key tolerance mechanism during *S. aureus* infection.

RESULTS

Autophagy Deficiency Results in Susceptibility to Systemic *S. aureus* Infection in a Strain-Specific Manner

To investigate the role of autophagy during *S. aureus* bacteremia, $Atg16L1^{HM}$ and wild-type (WT) control mice were intravenously (i.v.) infected with three different MRSA strains, USA300 (strain LAC), USA500 (strain 2395), and USA400 (strain MW2). $Atg16L1^{HM}$ mice displayed increased or accelerated lethality when infected with USA300 and USA500, but showed similar survival when infected with USA400 (Figure 1A, 1C–D). $LC3B^{-/-}$ mice are missing one of several paralogs of LC3, and therefore display a partial reduction in autophagy (Cann et al., 2008). We found that $LC3B^{-/-}$ mice also displayed enhanced lethality following i.v. infection with USA300 (Figure 1B). Thus, two distinct autophagy-deficient mouse lines are susceptible to this common MRSA strain that accounts for significant morbidity and mortality in humans (Gonzalez et al., 2006; Nimmo, 2012).

The increased lethality during USA300 infection observed in autophagy-deficient mice was unexpected based on the *in vitro* studies demonstrating that *S. aureus* subverts the autophagy pathway for intracellular survival (Mestre and Colombo, 2012; Mestre et al., 2010; Schnaith et al., 2007). To determine whether autophagy confers protection by promoting bacterial clearance, we quantified bacterial burden following USA300 infection of WT and Atg16L1^{HM} using the same conditions described above. Given that autophagy-deficiency could alter bacterial burden in a site-specific manner, we harvested blood, spleen, kidney, lungs, heart, liver, small intestine, cecal contents, colon, lymph nodes, and bladder. To ensure that we did not miss a transient difference in bacterial burden, tissue samples were harvested at a time point directly before the onset of lethality (day 3), a second time point when the first Atg16L1^{HM} mice die (day 4), and a third time point that examines surviving mice (day 7). We did not detect a significant difference in bacterial burden when comparing WT and Atg16L1^{HM} mice in any of these 33 conditions analyzed except a decrease in the intestinal contents of Atg16L1^{HM} mice on day 7 (Figure 2A–K). These results indicate that the enhanced lethality displayed by Atg16L1^{HM} mice is not associated with an increase in bacterial burden.

Next, we infected murine embryonic fibroblasts (MEFs) and peritoneal macrophages derived from WT and Atg16L1^{HM} mice with USA300 *in vitro*. Atg16L1-deficiency did not alter the amount of intracellular bacteria recovered from either cell type at any of the infectious doses or time points analyzed (Figure S1A–G). A previous study showed that Atg5$^{-/-}$ MEFs had decreased intracellular bacterial burden during infection with USA400 (Schnaith et al., 2007). However, we did not detect a difference in intracellular bacteria when we compared WT and Atg16L1^{HM} MEFs infected with USA400 (Figure S1H), potentially due to partial autophagy activity in these cells (Cadwell et al., 2008). Thus, our findings suggest that Atg16L1 provides protection against USA300 through a mechanism that does not involve reducing bacterial burden through degradation of internalized bacteria, consistent with the *in vivo* quantification of bacteria.

Autophagy Mediates Susceptibility to *S. aureus* Lung Infection

In addition to sepsis following blood infections, lung infection by USA300 has rapidly emerged as a significant cause of nosocomial pneumonia (Hageman et al., 2006; Pasquale et al., 2013). Thus, we utilized a previously described mouse model of pneumonia (Bubeck Wardenburg et al., 2007a) to determine whether autophagy deficiency increased susceptibility to lung infection. Following intranasal inoculation with USA300, Atg16L1^{HM} mice displayed increased morbidity and mortality compared with WT animals (Figure 3A–3B). The degree of histopathology in the lung was also more severe in Atg16L1^{HM} mice, which was characterized by signs of vascular damage such as thrombi in vessels, edema, and loss of integrity in the tissue architecture (Figure 3C–3F). Disease was not due to the procedure because all of the animals inoculated with an equal volume of PBS survived (Figure 3A). Consistent with a protective role for autophagy, LC3B$^{-/-}$ mice were also more susceptible to lethality following intranasal infection with USA300 compared with WT (Figure 3G).

Susceptibility to *S. aureus* Conferred by Autophagy Deficiency Is Dependent on α-toxin

S. aureus produces an incredible array of virulence factors that display a high degree of variability in expression. Such differences between strains may explain why Atg16L1^{HM} mice are susceptible to i.v injection with USA300 and USA500, but not USA400. Many of the virulence factors encoded by *S. aureus* are regulated by a quorum sensing two-component system known as the accessory gene regulator, encoded by the *agr* locus (Novick and Geisinger, 2008). We therefore infected Atg16L1^{HM} and WT mice with an isogenic strain of USA300 in which the *agr* locus is deleted (USA300 Δ*agr*), resulting in decreased production of many bacterial virulence factors. Using the same 1x10^{7} cfu dose as in previous experiments, USA300 Δ*agr* was unable to induce mortality in either WT or Atg16L1^{HM} mice following i.v. injection (Figure 4A). Although these results suggest that *agr* is necessary for the increased susceptibility observed in autophagy-deficient mice, it is possible that a higher infectious dose is necessary to observe a role for Atg16L1. However, we were still unable to detect a role for Atg16L1 when mice were infected with a 10-fold higher dose of 10^{8} cfu USA300 Δ*agr*, as both WT and Atg16L1^{HM} mice displayed similar lethality (Figure 4A). These results raise the possibility that an *agr*-regulated virulence factor is involved in the increased susceptibility observed in autophagy-deficient mice.

Among the virulence factors regulated by *agr*, the membrane-perforating toxin α-toxin has been implicated in bacteremia and pneumonia (Berube and Bubeck Wardenburg, 2013). While USA300 and USA500 produce high amounts of α-toxin, USA400 secretes very low amounts of this toxin (Figure 4B). Thus, we next examined the role of α-toxin by infecting mice with an isogenic USA300 mutant that contains a deletion in the gene encoding α-toxin, *hla* (USA300 Δ*hla*). Remarkably, Atg16L1^{HM} mice infected i.v. with USA300 Δ*hla* displayed a survival advantage compared to WT mice rather than susceptibility, especially at the higher dose (Figure 4C–4D). Furthermore, a reduced amount of bacteria was recovered from intestinal tissue of Atg16L1^{HM} animals on day 3 post infection (Figure S2A–S2K), suggesting that enhanced survival during infection with USA300 Δ*hla* could be due to increased resistance to infection. When inoculated intranasally with 10^{8} cfu of USA300 Δ*hla*, neither WT nor Atg16L1^{HM} mice displayed lethality (Figure 4E). Importantly, complementing the USA300 Δ*hla* mutant strain with a plasmid overexpressing *hla* restored mortality in both WT and Atg16L1^{HM} animals (Figure 4E). Therefore, we conclude that Atg16L1-deficiency mediates susceptibility to both sepsis and pneumonia following *S. aureus* in a manner dependent on α-toxin.

Atg16L1 Deletion in Endothelial Cells, but Not Macrophages or Dendritic Cells, Contributes to Enhanced Lethality

α-toxin contributes to lethal sepsis and pneumonia by binding A Disintegrin and Metalloprotease 10 (Adam10) expressed on the surface of endothelial cells, epithelial cells, and monocytes (Becker et al., 2014; Powers et al., 2012). The vascular damage observed by histopathology analysis in Atg16L1^{HM} mice following intranasal infection (Figure 3C–3F) may be indicative of increased sensitivity of the endothelium to α-toxin. We investigated the role of Atg16L1 in endothelial cells during infection by breeding mice expressing Cre recombinase under control of the Tie2 promoter with mice that have a loxP-flanked *Atg16L1* allele (Atg16L1$^{fl/fl}$-Tie2Cre). Successful deletion of Atg16L1 in endothelial cells was

confirmed by Western blot (WB) analysis (Figure S3E). We found that Atg16L1$^{fl/fl}$-Tie2Cre mice were significantly more susceptible to lethality following infection by USA300 compared with Atg16L1$^{fl/fl}$ control mice in both the blood and lung infection models (Figure 5A and 5B). Cre expression driven by the Tie2 promoter has been reported to cause non-specific deletions of LoxP-flanked gene segments in hematopoietic cells. Although bone marrow chimeras are frequently used to address this issue, we could not employ this strategy because the process of generating chimeras (e.g. irradiation) altered the disease course (Figure S3A). As an alternate approach, we analyzed the susceptibility of mice in which Atg16L1 is deleted in key hematopoietic cell types known to be essential for defense against *S. aureus* in the time frame we have been examining.

Myeloid cells in particular may be relevant because Atg16L1 deletion in these cells leads to excess IL-1β production that mediates lethality in a model of intestinal injury (Saitoh et al., 2008). Additionally, α-toxin mediates lethality following intranasal infection in part by inducing IL-1β production upon binding Adam10 on myeloid cells (Becker et al., 2014). However, we did not detect increased IL-1β in Atg16L1^{HM} mice infected i.v. or intranasally with USA300 compared to similarly treated WT mice (Figure S3B–S3D). To further investigate the role of Atg16L1 in various leukocyte populations, we utilized mice in which Atg16L1 is deleted in myeloid cells (monocytes, macrophages, and neutrophils) or dendritic cells by breeding Atg16l1$^{fl/fl}$ mice with mice expressing the Cre recombinase under control of the lysozyme M promoter (Atg16L1$^{fl/fl}$-LyzCre mice) or CD11c promoter (Atg16L1$^{fl/fl}$-CD11cCre mice), respectively (Hubbard-Lucey et al., 2014; Marchiando et al., 2013). Neither Atg16L1$^{fl/fl}$-LyzCre or Atg16L1$^{fl/fl}$-CD11cCre mice displayed a difference in survival compared to Atg16L1$^{fl/fl}$ controls, while Atg16L1^{HM} mice included in this experiment as a positive control displayed increased lethality (Figure 5C). Thus, Atg16L1 deletion in myeloid and dendritic cells is not sufficient to mediate enhanced lethality.

Intranasal α-toxin Treatment Is Sufficient to Induce Increased Lethality in Autophagy-Deficient Mice

We next investigated whether α-toxin alone, independent of bacterial replication, is sufficient to induce increased lethality in autophagy-deficient mice. To isolate biologically active toxin, α-toxin was over-produced in an engineered strain of *S. aureus* deficient in production of key cytotoxins (Newman Δ*hla*/*hlg*/*lukAB*/*lukED;pvl*$^{-}$) (Reyes-Robles et al., 2013). We confirmed the presence of α-toxin in the filter-sterilized supernatant of the toxin-overexpressing strain and not in supernatant from the parental toxin-deficient strain that was prepared the same way (Figure S4A). Atg16L1^{HM} mice inoculated via the intranasal route with the α-toxin suspension described above were significantly more susceptible to lethality compared with WT animals (Figure 6A). This lethality was attributable to α-toxin because neither WT nor Atg16L1^{HM} mice displayed lethality following inoculation with the toxin-deficient supernatant (Figure 6A). The increased lethality of Atg16L1^{HM} mice inoculated with α-toxin was associated with increased protein in the bronchoalveolar lavage fluid, suggesting that autophagy protects against disruption of endothelial and epithelial barriers (Figure 6B and S4B). Because these results were obtained in the absence of intact bacteria, the protection conferred by autophagy cannot be through resistance.

In addition to direct cell lysis, α-toxin induces barrier disruption by promoting Adam10-induced cleavage of integrins E-cadherin and VE-cadherin on epithelial and endothelial cells, respectively (Inoshima et al., 2011; Powers et al., 2012). We analyzed E-cadherin cleavage because we were unable to detect sufficient amounts of VE-cadherin in lung tissue by WB to be able to examine cleavage. Consistent with the increased barrier dysfunction, Atg16L1^{HM} mice had significantly higher levels of cleaved E-cadherin in the lungs, while total full-length E-cadherin was similar to WT (Figure S4C–S4F). Additionally, we detected an increase in the number of TUNEL^{+} cells in lung sections prepared from Atg16L1^{HM} mice treated with α-toxin, indicative of increased cell death in autophagy-deficient conditions (Figure 6C). To identify the cells targeted by α-toxin, single cell suspensions of lung harvested from Atg16L1^{HM} and WT mice were labeled with propidium iodide (PI) following intranasal intoxication and analyzed by flow cytometry. A higher percentage of ICAM^{+}PECAM^{+} endothelial cells and EpCAM^{+} epithelial cells from Atg16L1^{HM} mice incorporated PI compared with WT (Figure 6D–6H). By comparison, only a small percentage of the CD45^{+} cells, representing the hematopoietic compartment, incorporated PI in either Atg16L1^{HM} or WT mice (Figure 6F). There was no difference in cell death between WT and Atg16L1^{HM} mice treated with toxin-deficient control supernatant (Figure 6G–6H). These results indicate that autophagy deficient epithelial and endothelial cells, but not hematopoietic cells, are more susceptible to α-toxin during intranasal intoxication.

Autophagy-Deficient Endothelial Cells Are More Susceptible to α-toxin *in vitro*

To directly test whether autophagy protects endothelial cells from α-toxin *in vitro*, primary endothelial cells were harvested from WT and Atg16L1^{HM} mice and maintained in culture (Figure S5A). Cell death and pore formation measured by ethidium bromide (EtBr) incorporation were used as markers for toxin sensitivity. Endothelial cells from Atg16L1^{HM} mice were significantly more susceptible to cell death induced by α-toxin compared to WT cells (Figure 7A). Also, Atg16L1-deficient endothelial cells treated with α-toxin, but not the control supernatant, incorporated high amounts of EtBr (Figure 7B and 7C). In contrast, peritoneal macrophages from WT and Atg16L1^{HM} mice displayed a similar degree of cell death when treated with α-toxin (Figure S5B), consistent with our findings *in vivo* indicating that autophagy-deficiency selectively affects endothelial and epithelial cells rather than leukocytes.

Altered Adam10 expression could explain the increased sensitivity of Atg16L1-deficient endothelial cells to α-toxin. Consistent with this possibility, WB analyses indicated that Atg16L1^{HM} endothelial cells, but not hematopoietic bone marrow cells, had a striking increase in Adam10 compared with WT cells (Figure 7D–7F). Immunofluorescence analysis confirmed the increase in Adam10 observed in Atg16L1^{HM} endothelial cells (Figure 7G–7H). *Adam10* mRNA levels were similar in WT and Atg16L1^{HM} endothelial cells, indicating that the increase in Adam10 protein was due to post-transcriptional regulation (Figure 7I).

To further implicate autophagy in the regulation of Adam10, primary endothelial cells from WT mice were analyzed for Adam10 protein levels under autophagy inducing or inhibiting conditions. Inhibition of late stage autophagy with ammonium chloride (NH_4Cl) or Lys05, a

hydroxychloroquine derivative (McAfee et al., 2012), resulted in increased levels of Adam10 (Figure 7J–7M). Conversely, serum starvation, a classic stimulus of autophagy, decreased Adam10 levels (Figure 7N–7O). Similarly, treatment with epirubicin, an anthracycline drug that induces autophagy (Figueiredo et al., 2013), also led to a decrease in Adam10 protein (Figure 7P–7Q). Epirubicin has been shown to protect against sepsis by inducing autophagy in the lung (Figueiredo et al., 2013). Thus, we next tested whether chemically inducing autophagy with epirubicin can protect against toxinosis. Remarkably, we found that epirubicin increased survival of WT animals inoculated intranasally with α-toxin (Figure 7R). When taken together, these results are consistent with a model in which autophagy inhibition in endothelial cells confers susceptibility to α-toxin, which is associated with altered Adam10 protein levels.

DISCUSSION

Despite the growing evidence that tolerance mechanisms are critical for host defense, specific pathways that mediate tolerance towards antibiotic-resistant bacteria have not been sufficiently examined. We show that disruption of the autophagy gene *Atg16L1*, and consequently autophagy, increases *S. aureus*-mediated lethality in a strain-dependent manner. During systemic and intranasal infections, this increase in lethality was not accompanied by a change in bacterial burden, suggesting that Atg16L1 deficiency impairs tolerance rather than resistance. Impaired tolerance in Atg16L1-deficient animals was dependent on a single virulence factor secreted by *S. aureus*, α-toxin. Remarkably, deletion of α-toxin in *S. aureus* resulted in reversal of susceptibility between WT and Atg16L1 mutant animals, indicating that in the absence of α-toxin, autophagy deficiency may actually be beneficial to the host. This observation is reminiscent of our previous finding demonstrating that Atg16L1 deficiency confers protection during *C. rodentium* infection by reducing bacterial burden (Marchiando et al., 2013). This reversal in susceptibility highlights the context-specific role of autophagy and underscores the contribution of pathogen-encoded factors in determining the outcome of inhibiting a host defense pathway.

Pathways that maintain cell homeostasis in response to internal and external stressors promote tolerance in response to infectious challenges in a variety of model organisms (Bessede et al., 2014; Ferreira et al., 2011; Richardson et al., 2010; Taillebourg et al., 2014). Thus, autophagy could contribute to tolerance as a major homeostatic pathway. Indeed, the transcriptional regulator of autophagy HLH-30 (TFEB in mammals) promotes survival in *C. elegans* infected with *S. aureus* without affecting bacterial burden (Visvikis et al., 2014). However, the mechanism by which HLH-30 is providing protection is unclear. Although tolerance is frequently enhanced by dampening inflammation, HLH-30 was shown to induce inflammatory cytokine expression. How does autophagy, a cellular pathway that typically enhances immune responses, promote tolerance instead of resistance? Rather than directly controlling cytokine expression, our results suggest that autophagy can protect cells that are vulnerable to damage caused by a pathogen-specific virulence mechanism. Atg16L1 deletion in endothelial cells, but not myeloid or dendritic cells, recapitulated the enhanced lethality observed in $Atg16L1^{HM}$ mice. Also, α-toxin promoted cell death preferentially in Atg16L1-deficient endothelial or epithelial cells from $Atg16L1^{HM}$ mice *in vitro* and *in vivo*. Thus, although autophagy in other cell types may also be important during *S. aureus*

infection, cells that maintain barrier function appear to be particularly sensitive to Atg16L1 deficiency in the presence of an α-toxin-producing strain. This increased susceptibility is consistent with increased levels of the toxin receptor Adam10 in Atg16L1-deficient endothelial cells. The finding that Atg16L1-deficiency increases Adam10 protein rather than transcript may be related to the protein turnover function of autophagy because we found that lysosomal inhibition leads to a similar accumulation of Adam10. Given the broad role of autophagy in remodeling the proteome (Mathew et al., 2014), it will be important to determine whether additional substrates of autophagy impact tolerance in a pathogen-specific manner.

Finally, a rigorous comparison of inbred mouse strains during cerebral malaria indicates that subtle differences in genetic susceptibility can favor tolerance at the cost of resistance, or vice versa (Raberg et al., 2007). Our finding that Atg16L1-deficiency reduces bacterial burden in the intestine, which is supported by our previous finding in the *C. rodentium* model, suggests that Atg16L1 can favor tolerance at the cost of resistance in certain conditions. Thus, preventing tissue damage caused by *S. aureus* (e.g., through Adam10 blockade (Inoshima et al., 2011)) may not necessarily select for resistant bacteria. Additionally, a threonine to alanine substitution (T300A) in Atg16L1 that exists at high frequency in the human population has been shown to destabilize the protein and increase the risk of developing inflammatory bowel disease, a disorder associated with loss of tolerance towards commensal bacteria in the intestine (Lassen et al., 2014). It is possible that mutations in autophagy genes influence outcomes during *S. aureus* infection in humans as well. However, our results in mice indicate that a host mutation that increases susceptibility to one strain of *S. aureus* could reduce susceptibility to another strain, depending on the levels of α-toxin-produced. Therefore, population genetic studies may require concurrent analyses of genetic variation among bacterial strains to successfully identify gene variants that mediate susceptibility. All together, our results identify a remarkably specific relationship between the host pathway of autophagy and a bacterial toxin that dictates tolerance towards one of the most significant modern pathogens.

EXPERIMENTAL PROCEDURES

Mice

Age and gender-matched 6–9 week old mice on a C57BL/6 background were used. $Atg16L1^{HM}$, $Atg16L1^{fl/fl}$-LyzCre, $Atg16L1^{fl/fl}$-CD11cCre mice were previously described (Hubbard-Lucey et al., 2014; Marchiando et al., 2013; Ramanan et al., 2014). WT refers to C57BL/6 mice purchased from Jackson Laboratory and bred onsite to generate animals for experimentation. $LC3B^{-/-}$ mice (originally from Jackson Laboratory) backcrossed to the C57BL/6 background were kindly provided by Skip Virgin (Washington University School of Medicine). $Atg16L1^{fl/fl}$-Tie2Cre mice were generated by breeding $Atg16L1^{fl/fl}$ mice with Tie2Cre mice from Jackson Laboratory. $Atg16L1^{fl/fl}$-LyzCre, $Atg16L1^{fl/fl}$-CD11cCre, and $Atg16L1^{fl/fl}$-Tie2Cre were compared to littermate Cre-negative $Atg16L1^{fl/fl}$ mice as controls. All animal studies were performed according to approved protocols by the NYU School of Medicine Institutional Animal Care and Use Committee (IACUC).

Bacterial strains and infections

Strains used in this study are described in the supplemental experimental procedures. To generate the USA300 Δ*hla* mutant strain, USA300-AH1263 (USA300 *ermS* LAC) was transduced with phage 80α containing *hla::erm*. The USA300 *hla* mutant strain was also transformed with the pOS1 vector (empty vector) and the pDU1212 plasmid (P_{hla}^{-}*hla*) (O'Reilly et al., 1986). Bacteria were cultured overnight from a single colony in 5ml Tryptic Soy Broth (TSB) with shaking at 37 °C. Cultures were diluted 1:100 in TSB (5ml for i.v. infection, 50ml for intranasal infection) and cultured shaking at 37 °C for an additional 3 hours until optical density at 600 nm was 1.5 (10^9 cfu/ml). Intravenous infection was performed via tail vein injection. Inoculum for intranasal infection was prepared as described previously (Bubeck Wardenburg et al., 2007b). Mice were anesthetized using 200μl Avertin. 20μl bacterial slurry was administered via the left nare, and animals were held upright for 1 minute post inoculation then laid prone to recover. Inoculum was quantified by plating serial dilutions on Mannitol Salt Agar plates (MSA, BD Biosciences). For *in vivo* epirubicin treatment, WT animals were injected i.p. with 0.6μg/g body weight epirubicin in PBS or vehicle only control immediately prior to intranasal inoculation with α-toxin.

α-toxin preparation

The Newman Δ*hla*/*hlg*/*lukAB*/*lukED;pvl*$^{-}$ strain (Reyes-Robles et al., 2013) was transformed with the pDU1212 (P_{hla}^{-}*hla*) plasmid (O'Reilly et al., 1986). Transformed bacteria (α-toxin^{+}) and the parental strain (α-toxin^{-} control) were cultured overnight in RPMI (Gibco) supplemented with 1% CAS amino acids, (RPMI/CAS) diluted 1:100, and grown at 37 °C with shaking for an additional 6 hours. Cultures were centrifuged for 15 minutes at 4,000rpm and 4 °C. Supernatants were filter-sterilized (0.22μm) and concentrated to 10x using Spin-X UF Concentrator tubes (Corning) at 4000rpm and 4°C for 80 minutes. Supernatants containing α-toxin and toxin-less control supernatants were aliquoted into one-time use stocks frozen at −80 °C.

Statistics

GraphPad Prism v6 was used for analysis. Differences between two groups were assessed by two-tailed unpaired t test. Analyses involving multiple comparisons were performed by an ANOVA with the Holm-Sidak test. Bacterial burden in tissue specimens did not display normal distribution and was analyzed by the non-parametric Wilcoxon-Mann-Whitney test, or Kruskal-Wallis test and Dunn's correction for multiple comparisons on log-transformed cfu values. Survival between groups of mice was analyzed by the log rank Mantel-Cox test.

Supplementary Material

Refer to Web version on PubMed Central for supplementary material.

Acknowledgments

We would like to thank Alejandra Mendoza and Susan Schwab for assistance with endothelial cell isolation, Michael Cammer for assistance with imaging, NYUSoM Flow Cytometry and Cell Sorting Center (5P30CA016087-33), NYUSoM IHC Core (supported in part by NYUCI center support grant P30 CA16087), and

NYUSoM Microcopy Core (RR023704-01A1). This work was supported by US National Institute of Health (NIH) grants R01 DK093668 (K.C.), Training Grant #5 T32 GM0738 (K.M.), AI100853 (K.M.), F30 DK098925 (K.M.); American Heart Association 12GRNT12030041 (K.C.); R01AI099394 (V.J.T.); R01AI105129 (V.J.T.); Training Grant T32 AI007180 (T.R.-R.); F31 AI112290 (T.R.-R.); and F32 AI098395 (F.A.). V.J.T. is a Burroughs Wellcome Fund Investigator in the Pathogenesis of Infectious Diseases.

References

Alonzo F 3rd, Torres VJ. The bicomponent pore-forming leucocidins of Staphylococcus aureus. Microbiology and molecular biology reviews : MMBR. 2014; 78:199–230. [PubMed: 24847020]

Ayres JS, Trinidad NJ, Vance RE. Lethal inflammasome activation by a multidrug-resistant pathobiont upon antibiotic disruption of the microbiota. Nature medicine. 2012; 18:799–806.

Becker RE, Berube BJ, Sampedro GR, DeDent AC, Bubeck Wardenburg J. Tissue-Specific Patterning of Host Innate Immune Responses by Staphylococcus aureus alpha-Toxin. Journal of innate immunity. 2014; 6:619–631. [PubMed: 24820433]

Berube BJ, Bubeck Wardenburg J. Staphylococcus aureus alpha-toxin: nearly a century of intrigue. Toxins. 2013; 5:1140–1166. [PubMed: 23888516]

Bessede A, Gargaro M, Pallotta MT, Matino D, Servillo G, Brunacci C, Bicciato S, Mazza EM, Macchiarulo A, Vacca C, et al. Aryl hydrocarbon receptor control of a disease tolerance defence pathway. Nature. 2014; 511:184–190. [PubMed: 24930766]

Bubeck Wardenburg J, Bae T, Otto M, Deleo FR, Schneewind O. Poring over pores: alpha-hemolysin and Panton-Valentine leukocidin in Staphylococcus aureus pneumonia. Nature medicine. 2007a; 13:1405–1406.

Bubeck Wardenburg J, Patel RJ, Schneewind O. Surface proteins and exotoxins are required for the pathogenesis of Staphylococcus aureus pneumonia. Infection and immunity. 2007b; 75:1040–1044. [PubMed: 17101657]

Cadwell K, Liu JY, Brown SL, Miyoshi H, Loh J, Lennerz JK, Kishi C, Kc W, Carrero JA, Hunt S, et al. A key role for autophagy and the autophagy gene Atg16l1 in mouse and human intestinal Paneth cells. Nature. 2008; 456:259–263. [PubMed: 18849966]

Cann GM, Guignabert C, Ying L, Deshpande N, Bekker JM, Wang L, Zhou B, Rabinovitch M. Developmental expression of LC3alpha and beta: absence of fibronectin or autophagy phenotype in LC3beta knockout mice. Developmental dynamics : an official publication of the American Association of Anatomists. 2008; 237:187–195. [PubMed: 18069693]

Ferreira A, Marguti I, Bechmann I, Jeney V, Chora A, Palha NR, Rebelo S, Henri A, Beuzard Y, Soares MP. Sickle hemoglobin confers tolerance to Plasmodium infection. Cell. 2011; 145:398–409. [PubMed: 21529713]

Figueiredo N, Chora A, Raquel H, Pejanovic N, Pereira P, Hartleben B, Neves-Costa A, Moita C, Pedroso D, Pinto A, et al. Anthracyclines induce DNA damage response-mediated protection against severe sepsis. Immunity. 2013; 39:874–884. [PubMed: 24184056]

Gomes LC, Dikic I. Autophagy in antimicrobial immunity. Molecular cell. 2014; 54:224–233. [PubMed: 24766886]

Gonzalez BE, Rueda AM, Shelburne SA 3rd, Musher DM, Hamill RJ, Hulten KG. Community-associated strains of methicillin-resistant Staphylococccus aureus as the cause of healthcare-associated infection. Infection control and hospital epidemiology : the official journal of the Society of Hospital Epidemiologists of America. 2006; 27:1051–1056.

Hageman JC, Uyeki TM, Francis JS, Jernigan DB, Wheeler JG, Bridges CB, Barenkamp SJ, Sievert DM, Srinivasan A, Doherty MC, et al. Severe community-acquired pneumonia due to Staphylococcus aureus, 2003–04 influenza season. Emerging infectious diseases. 2006; 12:894–899. [PubMed: 16707043]

He C, Wei Y, Sun K, Li B, Dong X, Zou Z, Liu Y, Kinch LN, Khan S, Sinha S, et al. Beclin 2 functions in autophagy, degradation of G protein-coupled receptors, and metabolism. Cell. 2013; 154:1085–1099. [PubMed: 23954414]

Hubbard-Lucey VM, Shono Y, Maurer K, West ML, Singer NV, Ziegler CG, Lezcano C, Motta AC, Schmid K, Levi SM, et al. Autophagy Gene Atg16l1 Prevents Lethal T Cell Alloreactivity Mediated by Dendritic Cells. Immunity. 2014

Inoshima I, Inoshima N, Wilke GA, Powers ME, Frank KM, Wang Y, Bubeck Wardenburg J. A Staphylococcus aureus pore-forming toxin subverts the activity of ADAM10 to cause lethal infection in mice. Nature medicine. 2011; 17:1310–1314.

Ju JS, Miller SE, Jackson E, Cadwell K, Piwnica-Worms D, Weihl CC. Quantitation of selective autophagic protein aggregate degradation in vitro and in vivo using luciferase reporters. Autophagy. 2009; 5:511–519. [PubMed: 19305149]

Kennedy AD, Bubeck Wardenburg J, Gardner DJ, Long D, Whitney AR, Braughton KR, Schneewind O, DeLeo FR. Targeting of alpha-hemolysin by active or passive immunization decreases severity of USA300 skin infection in a mouse model. The Journal of infectious diseases. 2010; 202:1050–1058. [PubMed: 20726702]

Klevens RM, Morrison MA, Nadle J, Petit S, Gershman K, Ray S, Harrison LH, Lynfield R, Dumyati G, Townes JM, et al. Invasive methicillin-resistant Staphylococcus aureus infections in the United States. JAMA : the journal of the American Medical Association. 2007; 298:1763–1771.

Lassen KG, Kuballa P, Conway KL, Patel KK, Becker CE, Peloquin JM, Villablanca EJ, Norman JM, Liu TC, Heath RJ, et al. Atg16L1 T300A variant decreases selective autophagy resulting in altered cytokine signaling and decreased antibacterial defense. Proceedings of the National Academy of Sciences of the United States of America. 2014; 111:7741–7746. [PubMed: 24821797]

Levine B, Kroemer G. Autophagy in the pathogenesis of disease. Cell. 2008; 132:27–42. [PubMed: 18191218]

Marchiando AM, Ramanan D, Ding Y, Gomez LE, Hubbard-Lucey VM, Maurer K, Wang C, Ziel JW, van Rooijen N, Nunez G, et al. A deficiency in the autophagy gene Atg16L1 enhances resistance to enteric bacterial infection. Cell host & microbe. 2013; 14:216–224. [PubMed: 23954160]

Mathew R, Khor S, Hackett SR, Rabinowitz JD, Perlman DH, White E. Functional role of autophagy-mediated proteome remodeling in cell survival signaling and innate immunity. Molecular cell. 2014; 55:916–930. [PubMed: 25175026]

McAfee Q, Zhang Z, Samanta A, Levi SM, Ma XH, Piao S, Lynch JP, Uehara T, Sepulveda AR, Davis LE, et al. Autophagy inhibitor Lys05 has single-agent antitumor activity and reproduces the phenotype of a genetic autophagy deficiency. Proceedings of the National Academy of Sciences of the United States of America. 2012; 109:8253–8258. [PubMed: 22566612]

Medzhitov R, Schneider DS, Soares MP. Disease tolerance as a defense strategy. Science. 2012; 335:936–941. [PubMed: 22363001]

Mestre MB, Colombo MI. cAMP and EPAC are key players in the regulation of the signal transduction pathway involved in the alpha-hemolysin autophagic response. PLoS pathogens. 2012; 8:e1002664. [PubMed: 22654658]

Mestre MB, Fader CM, Sola C, Colombo MI. Alpha-hemolysin is required for the activation of the autophagic pathway in Staphylococcus aureus-infected cells. Autophagy. 2010; 6:110–125. [PubMed: 20110774]

Nimmo GR. USA300 abroad: global spread of a virulent strain of community-associated methicillin-resistant Staphylococcus aureus. Clinical microbiology and infection : the official publication of the European Society of Clinical Microbiology and Infectious Diseases. 2012; 18:725–734.

Novick RP, Geisinger E. Quorum sensing in staphylococci. Annual review of genetics. 2008; 42:541–564.

O'Reilly M, de Azavedo JC, Kennedy S, Foster TJ. Inactivation of the alpha-haemolysin gene of Staphylococcus aureus 8325–4 by site-directed mutagenesis and studies on the expression of its haemolysins. Microbial pathogenesis. 1986; 1:125–138. [PubMed: 3508485]

Orvedahl A, MacPherson S, Sumpter R Jr, Talloczy Z, Zou Z, Levine B. Autophagy protects against Sindbis virus infection of the central nervous system. Cell host & microbe. 2010; 7:115–127. [PubMed: 20159618]

Pamplona A, Ferreira A, Balla J, Jeney V, Balla G, Epiphanio S, Chora A, Rodrigues CD, Gregoire IP, Cunha-Rodrigues M, et al. Heme oxygenase-1 and carbon monoxide suppress the pathogenesis of experimental cerebral malaria. Nature medicine. 2007; 13:703–710.

Pasquale TR, Jabrocki B, Salstrom SJ, Wiemken TL, Peyrani P, Haque NZ, Scerpella EG, Ford KD, Zervos MJ, Ramirez JA, et al. Emergence of methicillin-resistant Staphylococcus aureus USA300 genotype as a major cause of late-onset nosocomial pneumonia in intensive care patients in the

USA. International journal of infectious diseases : IJID : official publication of the International Society for Infectious Diseases. 2013; 17:e398–403. [PubMed: 23375542]

Powers ME, Kim HK, Wang Y, Bubeck Wardenburg J. ADAM10 mediates vascular injury induced by Staphylococcus aureus alpha-hemolysin. The Journal of infectious diseases. 2012; 206:352–356. [PubMed: 22474035]

Raberg L, Graham AL, Read AF. Decomposing health: tolerance and resistance to parasites in animals. Philosophical transactions of the Royal Society of London Series B, Biological sciences. 2009; 364:37–49.

Raberg L, Sim D, Read AF. Disentangling genetic variation for resistance and tolerance to infectious diseases in animals. Science. 2007; 318:812–814. [PubMed: 17975068]

Ramanan D, Tang MS, Bowcutt R, Loke P, Cadwell K. Bacterial Sensor Nod2 Prevents Inflammation of the Small Intestine by Restricting the Expansion of the Commensal Bacteroides vulgatus. Immunity. 2014; 41:311–324. [PubMed: 25088769]

Reyes-Robles T, Alonzo F 3rd, Kozhaya L, Lacy DB, Unutmaz D, Torres VJ. Staphylococcus aureus leukotoxin ED targets the chemokine receptors CXCR1 and CXCR2 to kill leukocytes and promote infection. Cell host & microbe. 2013; 14:453–459. [PubMed: 24139401]

Richardson CE, Kooistra T, Kim DH. An essential role for XBP-1 in host protection against immune activation in C. elegans. Nature. 2010; 463:1092–1095. [PubMed: 20182512]

Rodvold KA, McConeghy KW. Methicillin-resistant Staphylococcus aureus therapy: past, present, and future. Clinical infectious diseases : an official publication of the Infectious Diseases Society of America. 2014; 58(Suppl 1):S20–27. [PubMed: 24343828]

Saitoh T, Fujita N, Jang MH, Uematsu S, Yang BG, Satoh T, Omori H, Noda T, Yamamoto N, Komatsu M, et al. Loss of the autophagy protein Atg16L1 enhances endotoxin-induced IL-1beta production. Nature. 2008; 456:264–268. [PubMed: 18849965]

Sampedro GR, DeDent AC, Becker RE, Berube BJ, Gebhardt MJ, Cao H, Bubeck Wardenburg J. Targeting Staphylococcus aureus alpha-Toxin as a Novel Approach to Reduce Severity of Recurrent Skin and Soft-Tissue Infections. The Journal of infectious diseases. 2014; 210:1012–1018. [PubMed: 24740631]

Schnaith A, Kashkar H, Leggio SA, Addicks K, Kronke M, Krut O. Staphylococcus aureus subvert autophagy for induction of caspase-independent host cell death. The Journal of biological chemistry. 2007; 282:2695–2706. [PubMed: 17135247]

Schneider DS, Ayres JS. Two ways to survive infection: what resistance and tolerance can teach us about treating infectious diseases. Nature reviews Immunology. 2008; 8:889–895.

Stryjewski ME, Corey GR. Methicillin-resistant Staphylococcus aureus: an evolving pathogen. Clinical infectious diseases : an official publication of the Infectious Diseases Society of America. 2014; 58(Suppl 1):S10–19. [PubMed: 24343827]

Taillebourg E, Schneider DS, Fauvarque MO. The Drosophila Deubiquitinating Enzyme dUSP36 Acts in the Hemocytes for Tolerance to Listeria monocytogenes Infections. Journal of innate immunity. 2014; 6:632–638. [PubMed: 24777180]

Vandenesch F, Lina G, Henry T. Staphylococcus aureus hemolysins, bi-component leukocidins, and cytolytic peptides: a redundant arsenal of membrane-damaging virulence factors? Frontiers in cellular and infection microbiology. 2012; 2:12. [PubMed: 22919604]

Visvikis O, Ihuegbu N, Labed SA, Luhachack LG, Alves AM, Wollenberg AC, Stuart LM, Stormo GD, Irazoqui JE. Innate host defense requires TFEB-mediated transcription of cytoprotective and antimicrobial genes. Immunity. 2014; 40:896–909. [PubMed: 24882217]

Wang C, Mendonsa GR, Symington JW, Zhang Q, Cadwell K, Virgin HW, Mysorekar IU. Atg16L1 deficiency confers protection from uropathogenic Escherichia coli infection in vivo. Proceedings of the National Academy of Sciences of the United States of America. 2012; 109:11008–11013. [PubMed: 22715292]

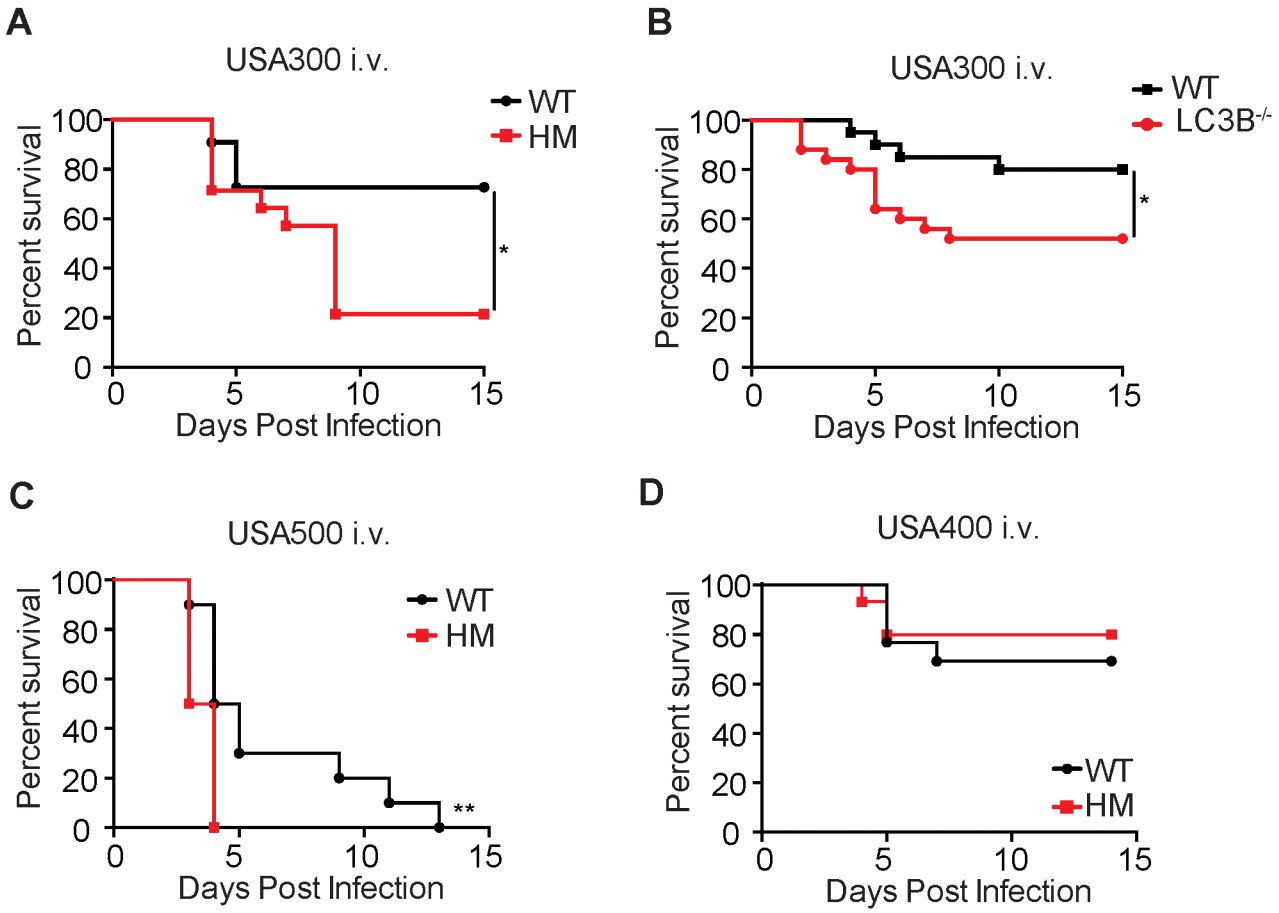

Figure 1. Autophagy Deficiency Results in Susceptibility to Systemic *S. aureus* Infection in a Strain-Specific Manner

(A) Survival curve of wild-type control (WT) and Atg16L1 hypomorph (HM) mice infected i.v. with 10^7 colony forming units (cfu) USA300. *n*=12–14 mice/group.

(B) Survival curve of WT and LC3B$^{-/-}$ mice infected with 10^7 cfu USA300. *n*=20–25 mice/group.

(C) Survival curve of WT and Atg16L1^{HM} mice infected with 10^7 cfu USA500. *n*=10 mice/group.

(D) Survival curve of WT and Atg16L1^{HM} mice infected with 10^7 cfu USA400. *n*=15 mice/group.

Data represent at least 2 independent repeats. *p<0.05, **p<0.01

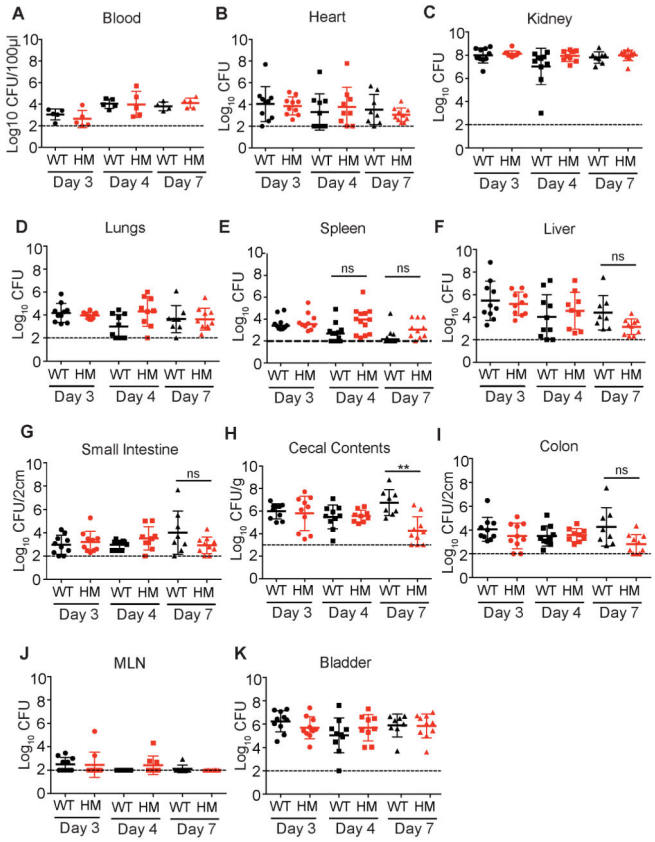

Figure 2. WT and Atg16L1^{HM} mice display similar bacterial burden during *S. aureus* infection

(A–K) Bacterial burden was quantified in the indicated organs and blood harvested from WT and Atg16L1^{HM} mice injected i.v. with 10^7 cfu USA300 on days 3, 4, and 7 post infection. Data points represent bacterial burden in individual mice, bars represent median, and dashed line represents limit of detection. *n*=8–13 mice/condition. No significant differences in bacterial burden were noted when comparing the same organ from WT and Atg16L1^{HM} mice except when comparing cecal contents on day 7 (H). Statistical analyses were performed by ANOVA with the Kruskal-Wallis test and Dunn's correction. Each time point represents data pooled from 2–3 independent repeats.

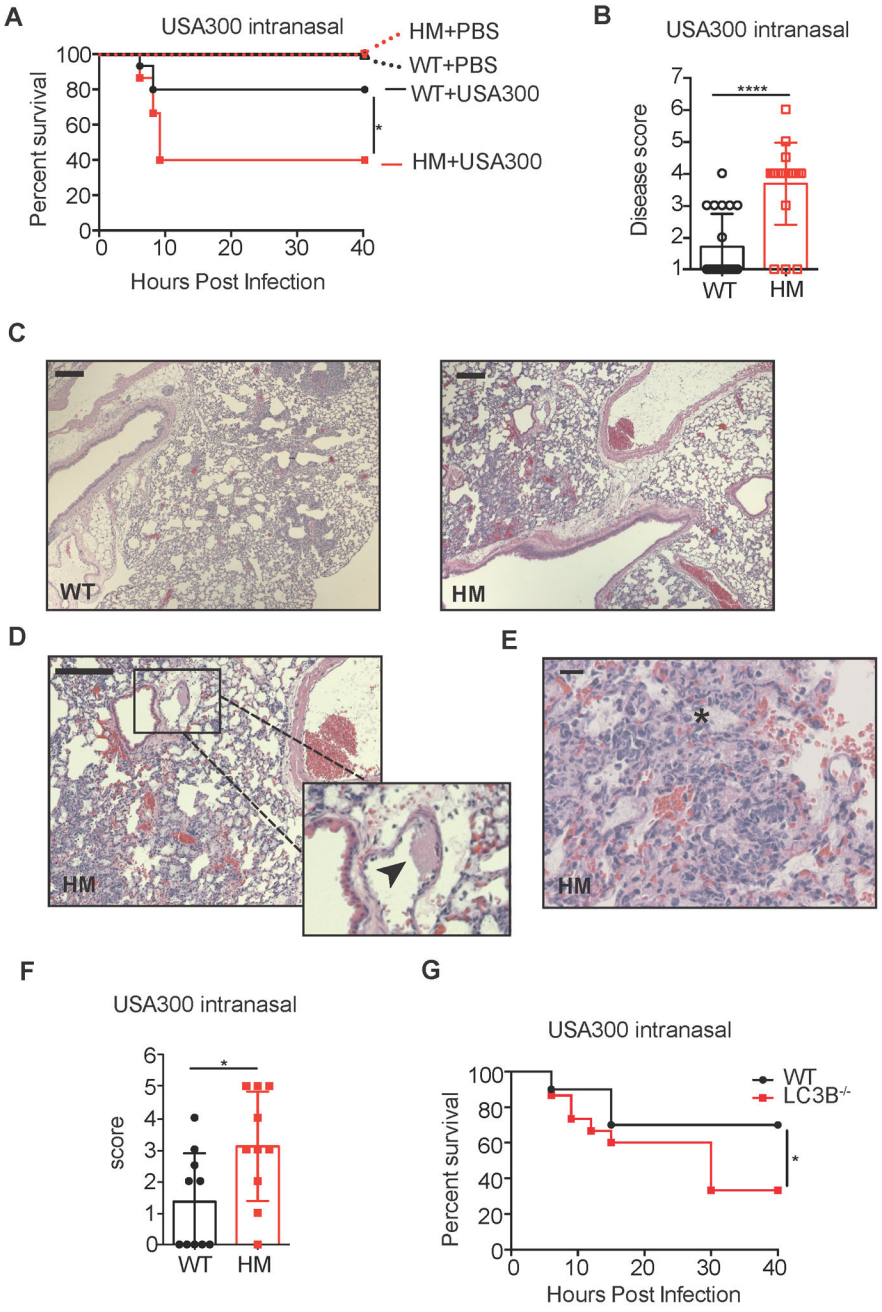

Figure 3. Autophagy Mediates Susceptibility to *S. aureus* Lung Infection

(A) Survival curve of WT and Atg16L1^{HM} mice inoculated intranasally with 4x10^{8} cfu USA300 or equivalent volume of PBS. *n*=15 mice/group for USA300 and *n*=5 mice/group for PBS.

(B) Disease score of WT and Atg16L1^{HM} mice 6 hours post intranasal inoculation with 4x10^{8} cfu USA300. Disease score was calculated using a 7-point activity assessment score based on mobility, food and water intake, posture, and fur ruffling (see supplemental methods). *n*=10 mice/group. Data represent mean and SEM.

(C) Representative H&E-stained sections of lungs from WT and Atg16L1^{HM} mice 6 hr post intranasal inoculation with 4x10^{8} cfu USA300. scale bar = 200 μm.
(D–E) Higher magnification images showing features only present in the lungs from Atg16L1^{HM} mice. Black arrow head in (D) indicates fibrin thrombus and asterisk in (E) indicates edema. scale bar = 200 μm (D) or 20 μm (E).
(F) Blind quantification of pathology observed in lungs from WT and Atg16L1^{HM} mice. Score was calculated using a 5-point score based on tissue destruction, hemorrhage, and visible cocci (see supplemental methods). n=10 mice/group. Data represent mean and SEM.
(G) Survival curve of WT and LC3B$^{-/-}$ mice inoculated intranasally with 4x10^{8} cfu USA300. *n*=15–20 mice/group.
Data represent at least 2 independent experiments. *p<0.05, ****p<0.0001

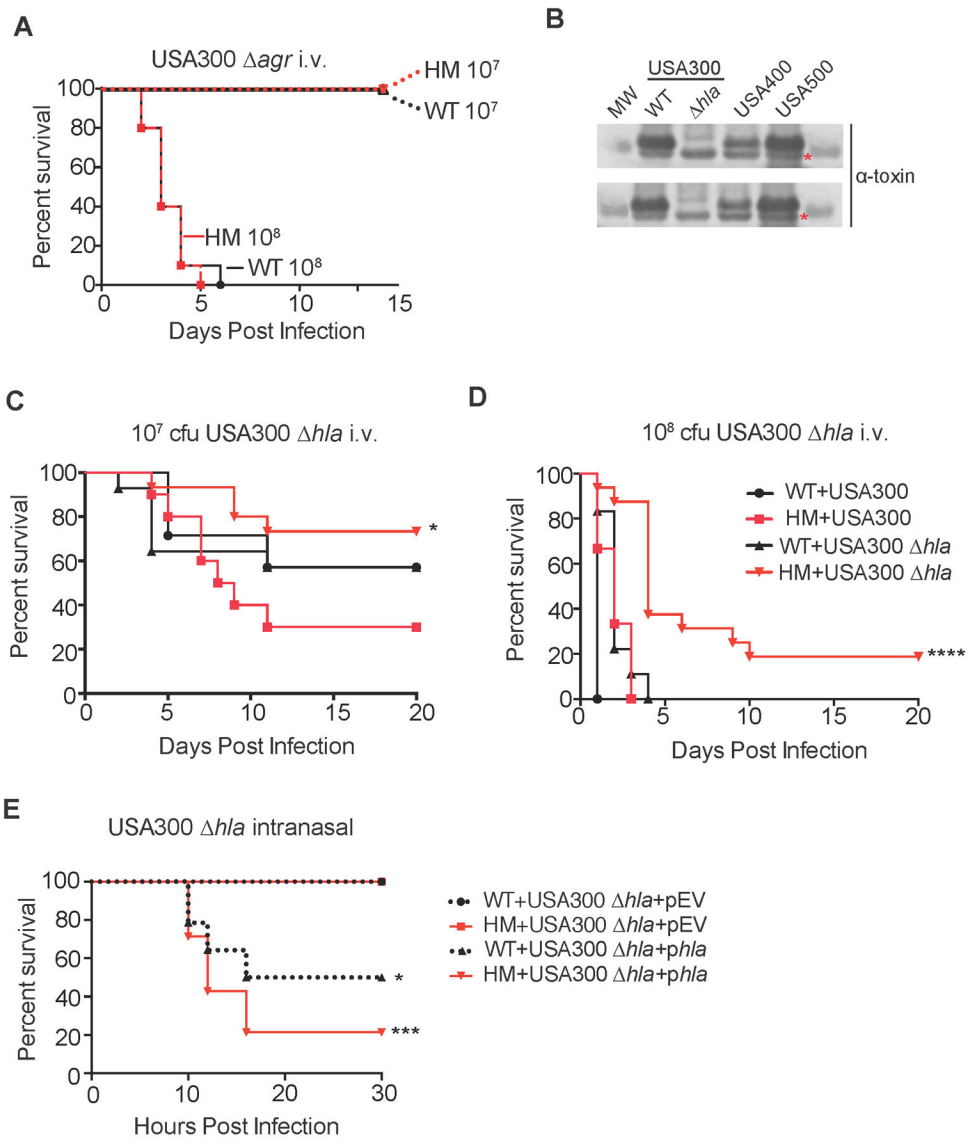

Figure 4. Susceptibility to *S. aureus* Conferred by Autophagy Deficiency Is Dependent on Bacterial α-toxin Production

(A) WT and Atg16L1^{HM} mice were injected i.v. with 10^7 or 10^8 cfu USA300 Δ*agr*. *n*=10 mice/group. Data represent 2 independent experiments.

(B) Western blot analysis of USA300, USA300 Δ*hla*, USA400, and USA500 using an anti-α-toxin antibody. MW indicates molecular weight protein marker, WT indicates isogenic wild type USA300, asterisk indicates a non-specific, anti-α-toxin cross-reactive band.

(C) WT and Atg16L1^{HM} mice were infected i.v. with 10^7 cfu USA300 or USA300 Δ*hla*. *n*=7–15 mice/group. Data represent 2 independent experiments. *p<0.05 comparing Atg16L1^{HM} + USA300 versus Atg16L1^{HM} + USA300 Δ*hla*.

(D) WT and Atg16L1^{HM} mice were infected i.v. with 10^8 cfu USA300 or USA300 Δ*hla*. *n*=7–15 mice/group. Data represent 4 independent experiments. ****p<0.0001 comparing Atg16L1^{HM} + USA300 versus Atg16L1^{HM} + USA300 Δ*hla* and ****p<0.0001 comparing Atg16L1^{HM} + USA300 Δ*hla* versus WT + USA300 Δ*hla*.

(E) WT and Atg16L1^{HM} mice were inoculated intranasally with 10^8 cfu USA300 Δ*hla* transformed with either empty plasmid (USA300 Δ*hla*+EV) or a plasmid overexpressing *hla* (USA300 Δ*hla*+p*hla*). *n*=8–14 mice/group. Data represent 3 independent experiments. *p<0.05 comparing WT + USA300 Δ*hla*+EV with WT + USA300 Δ*hla*+p*hla*. ***p<0.001 comparing Atg16L1^{HM} + USA300 Δ*hla*+EV with Atg16L1^{HM} + USA300 Δ*hla*+p*hla*.

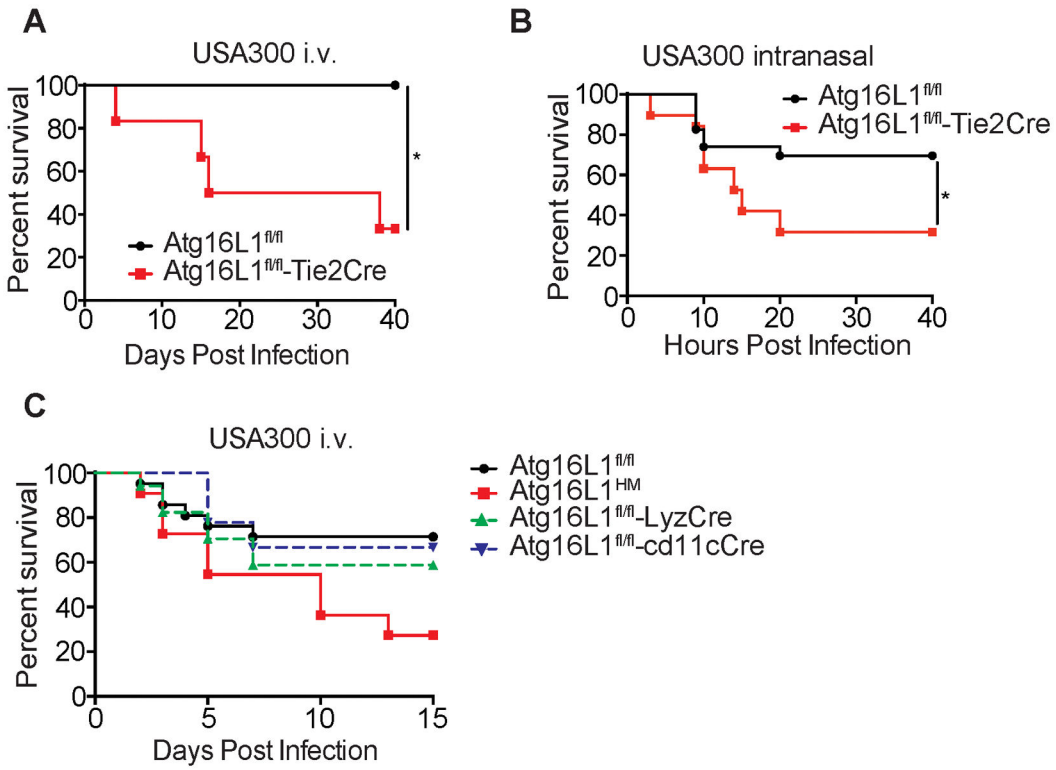

Figure 5. Atg16L1 Deletion in Endothelial Cells Confers Susceptibility to *S. aureus* Mediated Lethality

(A) Survival curve of Atg16L1$^{fl/fl}$ (controls) and Atg16L1$^{fl/fl}$-Tie2Cre mice infected i.v. with 10^7 cfu USA300. *n*=5–6 mice/group.

(B) Survival curve of Atg16L1$^{fl/fl}$ and Atg16L1$^{fl/fl}$-Tie2Cre mice inoculated intranasally with $4x10^8$ cfu USA300. *n*=24 mice for Atg16L1$^{fl/fl}$ and *n*=15 mice for Atg16L1$^{fl/fl}$ -Tie2Cre.

(C) Survival curve of Atg16L1^{HM}, Atg16L1$^{fl/fl}$, Atg16L1$^{fl/fl}$-LyzCre, and Atg16L1$^{fl/fl}$-CD11cCre mice infected i.v. with 10^7 cfu USA300. *n*=10 mice for Atg16L1^{HM}, *n*=21 mice for Atg16L1$^{fl/fl}$, *n*=18 mice for Atg16L1$^{fl/fl}$-LyzCre, *n*=9 mice for Atg16L1$^{fl/fl}$-CD11cCre. Data represent at least 2 independent experiments. *p<0.05

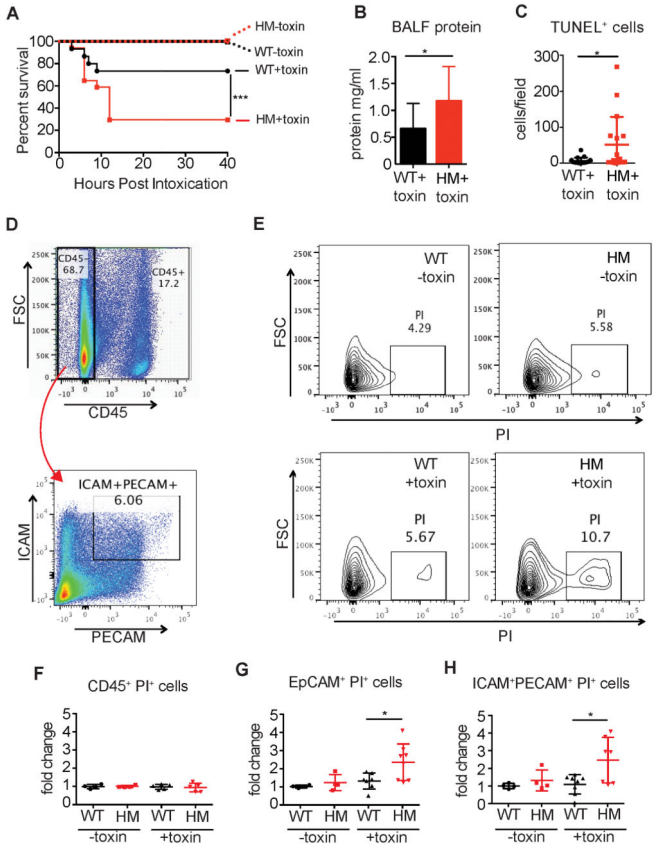

Figure 6. Intranasal α-toxin Treatment Is Sufficient to Induce Increased Lethality in Atg16L1-Deficient Mice

(A) Survival curve of WT and Atg16L1^{HM} mice inoculated intranasally with a 20μl suspension of filter-sterilized *S. aureus* culture supernatant containing α-toxin (+toxin) or lacking α-toxin (toxin). Supernatant were prepared from the exotoxin-deficient Newman Δ*hla*/*hlg*/*lukAB*/*lukED*/*pvl*& strain +/− α-toxin overexpression. *n*=15–17 mice/group.

(B) Protein content of bronchoalveolar lavage fluid of WT and Atg16L1^{HM} mice 3 hours post-intranasal inoculation with α-toxin as in (A). *n*=12–13 mice/group. Data points represent mean and SEM.

(C) Quantification of TUNEL^{+} cells per field of WT and Atg16L1^{HM} mice 3 hours post-intranasal inoculation with α-toxin as in (A). *n*=3 mice/group. Data points represent mean and SEM.

(D–H) Flow cytometry analysis of single cell lung homogenates from WT and Atg16L1^{HM} mice 3 hours post-intranasal inoculation with α-toxin.

(D) Plots showing gating strategy to identify ICAM^{+}PE-CAM^{+} cells within the CD45^{-} fraction. Representative WT mouse shown.

(E) Representative plots of PI^{+} cells gated on the CD45^{-}ICAM^{+}PE-CAM^{+} fraction as in (D) from lungs harvested from mice treated with α-toxin (bottom panels) or control suspension (top panels). Samples harvested from WT and Atg16L1^{HM} mice are represented in the left and right panels, respectively.

(F–H) Quantification of the proportion of (F) $CD45^+$, (G) $CD45^-EpCam^+$, and (H) $CD45^-ICAM^+PE\text{-}CAM^+$ cells that are PI^+ 3 hours post-intranasal inoculation with α-toxin or control suspension. Values are expressed as fold-change over WT mice treated with control suspension. *n*=4–7 mice/group

Individual points in (B), (C), (F), (G), and (H) represent cells from individual animals and bar graphs in (B) represent mean and SEM from at least two independent experiments. *p<0.05, **p<0.01, ***p<0.001

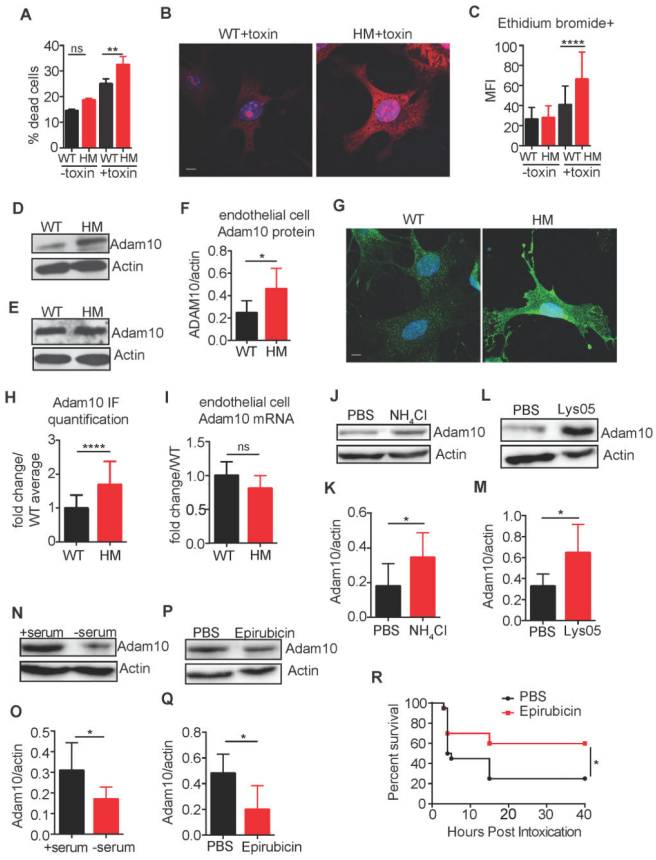

Figure 7. Autophagy-Deficient Endothelial Cells Are More Susceptible to α-toxin *in vitro*.

(A) Percent cell death measured by the lactate dehydrogenase (LDH) assay in cultured endothelial cells harvested from WT and Atg16L1^{HM} mice inoculated with α-toxin or control suspension. Data represents 5 independent experiments, each using cells pooled from 2 WT or Atg16L1^{HM} mice. Data represent mean and SEM.

(B) Representative images of ethidium bromide incorporation by endothelial cells from WT and Atg16L1^{HM} mice inoculated with α-toxin as an assay for pore formation. Scale bar=10μm.

(C) Quantification of mean fluorescent intensity (MFI) per cell from (B). *n*=44 cells from 3 WT mice and 83 cells from 3 Atg16L1^{HM} mice. Data represent mean and SEM.

(D–F) Representative Western blots for Adam10 and actin in whole cell lysates prepared from endothelial cells (D) and bone marrow cells (E) harvested from WT and Atg16L1^{HM} mice. Quantification of Adam10 levels normalized to actin in endothelial cells shown in (F). *n*=5–6 mice/group. Data represent mean and SEM.

(G) Representative immuno-fluorescence staining of Adam10 in endothelial cells from WT and Atg16L1^{HM} mice. Scale bar=10μm.

(H) Quantification of mean fluorescent intensity (MFI) per cell from (E). *n*=63 cells from 3 WT mice and 137 cells from 3 Atg16L1^{HM} mice. Data represent mean and SEM.

(I) *Adam10* mRNA expression in endothelial cells from WT and Atg16L1^{HM} mice normalized to *GAPDH*. *n*=5 mice/group.

(J–K) Representative Western blot (J) and quantification (K) for Adam10 and actin in whole cell lysates from WT endothelial cells treated with PBS or 20mM ammonium chloride (NH_4Cl) for 24 hours. *n*=7 replicates/group from 2 independent experiments (see supplemental methods for full experimental design).

(L–M) Representative Western blot (L) and quantification (M) for Adam10 and actin in whole cell lysates from WT endothelial cells treated with PBS 5μM Lys05 for 24 hours. *n*=6–9 replicates/group from 2 independent experiments.

(N–O) Representative Western blot (N) and quantification (O) for Adam10 and actin in whole cell lysates from WT endothelial cells treated with complete media (+serum) or media without serum (− serum) for 6 hours to induce autophagy. *n*=6–7 replicates/group from 2 independent experiments.

(P–Q) Representative Western blot (P) and quantification (Q) for Adam10 and actin in whole cell lysates from WT endothelial cells treated with PBS or 100μM epirubicin for 6 hours. *n*=4–5 replicates/group from 2 independent experiments.

(R) Survival curve of curve of WT mice treated i.p. with epirubicin (0.6μg/g body weight) or PBS vehicle control and inoculated intranasally with a 20μl suspension of filter-sterilized *S. aureus* culture supernatant containing α-toxin (+toxin). *n*=19–20 from 4 independent experiments.

*p<0.05, **p<0.01, ****p<0.0001